

AUTHORS



DIPL.-ING. STEPHAN KASPAR
 is Ph.D. Student with the team "Active Chassis Control" within BMW Group Research and Technology in Munich (Germany).



DR.-ING. RALF STROPH
 is Development Engineer with the team "Active Chassis Control" within BMW Group Research and Technology in Munich (Germany).



DR.-ING. TILMAN BÜNTE
 is Research Associate at the Institute of System Dynamics and Control within the German Aerospace Center (DLR) in Oberpfaffenhofen (Germany).



PROF. DR.-ING. SÖREN HOHMANN
 is Full Professor with the Institute of Control Systems within the Institute of Technology in Karlsruhe (Germany).

OPTIMISATION OF VEHICLE DYNAMICS VIA TORQUE VECTORING FOR SPACE OPTIMISED ELECTRIC VEHICLES

Available space optimised packaging of the drivetrain components can lead to unconventional wheel axle loads, which have to be taken into account for the design of the vehicles' dynamics. The BMW Group Research and Technology developed in cooperation with the German Aerospace Institute (DLR) and the Institute of Control Systems (IRS) within the Karlsruhe Institute of Technology (KIT) a control concept for torque vectoring. In spite of the challenge of high rear axle loads, attractive and at the same time safe ride characteristics are achieved by utilisation of independent distribution of drive and brake wheel torques.



1	INTRODUCTION
2	FUNCTIONAL STRUCTURE
3	SIMULATION RESULTS
4	CONCLUSION AND OUTLOOK

1 INTRODUCTION

When newly designing electric vehicles it is not sufficient to simply revert to a conventional vehicle layout and replace the combustion engine by an electric engine. Instead, boundary conditions have to be taken into account and the innovative degrees of freedom given by electro mobility must be used and converted into new vehicle concepts [1, 2] to work out the area of conflict between costs, weight, performance and installation space requirements.

Common concepts for electric vehicles are either equipped with a centrally arranged power unit or are carried out as decentralised in-wheel multi motor concepts. Drivetrain layouts with centralised single engines cannot provide additional installation space due to common arrangement of gears, differential, axes and drive shafts. However, making use of decentralised drivetrain design leads to a space-saving arrangement of high-voltage batteries, electric engines and gears in the well protected rear end of the vehicle for optimal utilisation of installation space. On a less positive note, resulting heavy rear axle loads connote a challenging issue in matters of driving dynamics. Commonly accepted solutions are mixed tyres and a firm chassis set-up. The possibility of independently distributing drive and brake wheel torques creates an additional degree of freedom for the control of driving dynamics, which can be used to stabilise the vehicle, as well as for agilisation [3]. This ultimately leads to improvement of desirability of electric vehicles with unconventional vehicle genes together with a maximisation of driving safety [4]. A few conventional vehicle concepts provide the opportunity of a mechanical torque vectoring. Mostly, due to efficiency reasons (amongst others), torque vectoring has to be activated by driving situation detection [5] and overstepping of specified thresholds [6]. For an electric single wheel drive, a continuous control intervention is feasible [7, 8] as the electric motors are continuously controlled anyways.

According to this, improvement of driving performance of a vehicle concept with electric single wheel drives attached to the rear wheel axle in combination with increased rear axle load is investigated within this contribution. Technical data is given in ❶.

2 FUNCTIONAL STRUCTURE

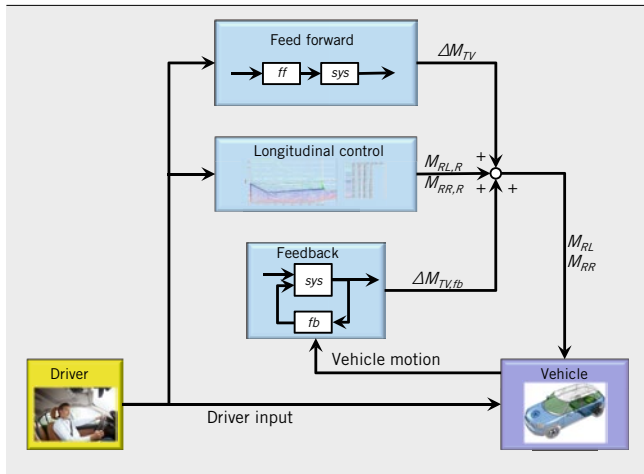
Systematic override of the vehicles' driving behaviour via torque vectoring is carried out by a collaboration of BMW, DLR and KIT, ❷. The desired vehicle acceleration is evaluated in the block longitudinal control based on drive pedal and brake pedal angles in the longitudinal control unit, which is converted into an equally distributed wheel torque left and right. For safety reasons, brake pedal input is always given top priority. Brake force distribution is chosen in terms of optimised recuperation in consideration of driving dynamics boundary conditions.

Additively, an additional difference wheel torque is superimposed, which is similar according to its amount but with unlike signs left

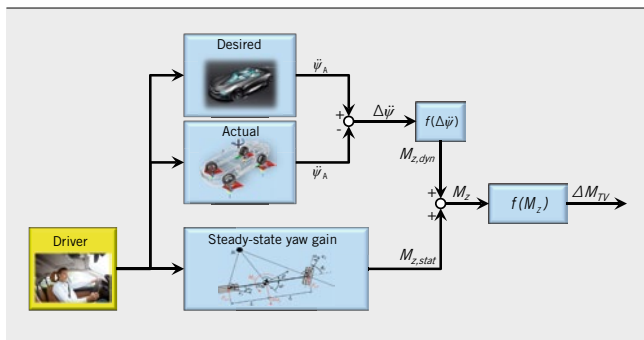
TECHNICAL DATA OF THE VEHICLE CONCEPT

Effective power	2 × 60 kW
Peak power	2 × 120 kW
Vehicle mass	1700 kg
Battery capacity	20 kWh
Maximum speed	150 kph
Maximum wheel torque	1400 Nm
Axle load distribution FA:RA	40:60
Drivetrain layout	Rear wheel drive

❶ Technical data



2 Wheel torque control block diagram



3 Functional architecture of the feed forward control

and right. By this means, yawing dynamics are modified without influencing longitudinal movement. Calculation of the additional torque is made via a combination of model-based feed forward and yaw rate feedback control. The feedback part is only held available for elimination of model inaccuracies and disturbances. When designing the feedback control one has to take care that it is robust against disturbances, but fast enough to eliminate deviations from

the nominal value. Results within this work are achieved only by activation of the feed forward part without feedback control.

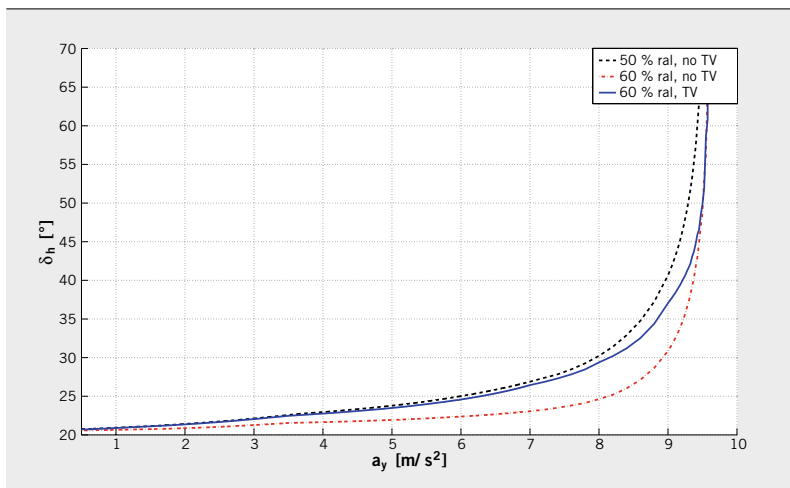
The feed forward control consists of two parts, one steady-state and one dynamic, 3. Decoupling of those input requirements gives way for additional degrees of freedom for vehicle dynamics design [9]. In that way, steady-state driving behaviour can be adjusted towards more understeering while independently enhancing agility for transient manoeuvres. Both parts of the feed forward control are based on two single track models: One to specify the vehicles' desired characteristics, and another single track model, which is enhanced by an external yaw moment, for emulation of the actual vehicle behaviour. To evaluate the static behaviour and with this the steady-state yaw gain, the equations of the single track models are solved for steady-state assumptions. In this way, an additional external yaw moment is calculated for obtaining the desired steady-state yaw rate. For transient nominal values of the yaw rate, this consideration itself is insufficient. Therefore, two single track models are computed in real-time to calculate the desired and actual yaw accelerations $\dot{\psi}$. The resulting difference of yaw accelerations is finally transformed into a corresponding differential wheel torque to provide the desired yaw rate even for transient courses of the steering wheel angle.

3 SIMULATION RESULTS

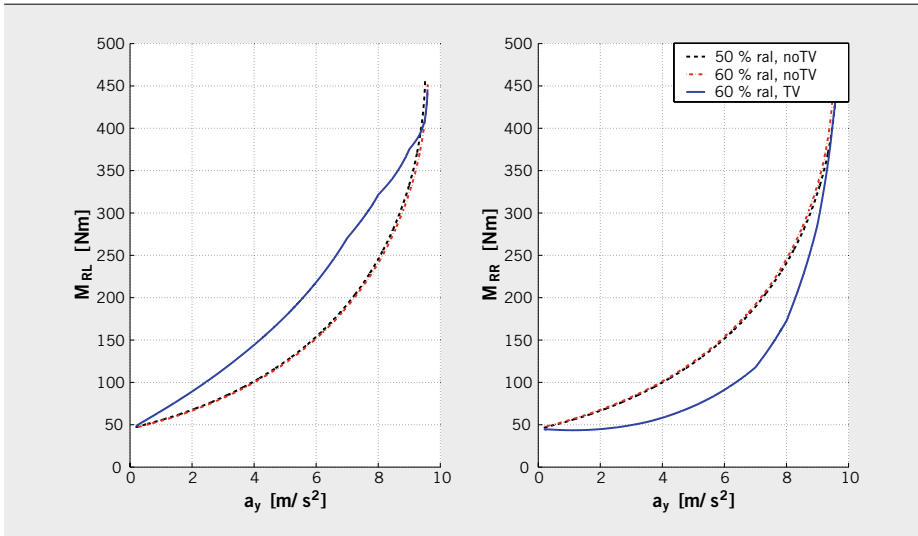
Investigation on handling and road behaviour is made through simulation, using a Matlab/Simulink-based vehicle model with 5 bodies and 16 degrees of freedom. Tyre forces are calculated through a bench test parameterised magic formula tyre model according to Pacejka [10]. Kinematic dependencies are determined by virtual calculation primary and refined through bench test measurements afterwards. For pointing out the potential in terms of driving dynamics, no system limits are taken into account. Nevertheless, demands on wheel torques stay within feasible bounds of potential electric drive concepts.

3.1 QUASI STEADY-STATE CORNERING

Steady-state driving behaviour is usually examined through the closed-loop manoeuvre quasi steady-state cornering. Within this manoeuvre, the car is driving in a circle with a constant radius. Chosen acceleration is very small so that the lateral acceleration



4 Steering wheel angle versus lateral acceleration for quasi steady-state cornering



5 Wheel torques left and right versus lateral acceleration for quasi steady-state cornering

CHARACTERISTIC VALUE	CALCULATION	50 % RAL, NO TV	60 % RAL, NO TV	60 % RAL, TV
T_{ψ} [s]	$T_{\psi 90\%} - T_{\delta H, 50\%}$	0.11	0.12	0.10
OS_{ψ} [-]	$\frac{\dot{\psi}_{\max} - \dot{\psi}_{\text{stat}}}{\dot{\psi}_{\text{stat}}}$	0.115	0.094	0.077

6 Characteristic values for the step-steer manoeuvre

slowly increases while the influence by longitudinal tyre forces is kept at a minimum. The yaw acceleration is around $0.6 \text{ }^\circ/\text{s}^2$ so that a quasi steady-state conditions are obtained and evaluation can be made according to [11].

Decisive for this manoeuvre is the course of the steering wheel angle δ_{SWA} versus lateral acceleration a_y . It should be mildly linear increasing at the beginning and heavily rising for higher lateral accelerations for giving notice to the driver of approaching driving dynamics limits. Oversteer situations, which can be determined by the decrease of the steering wheel angle, have to be absolutely avoided.

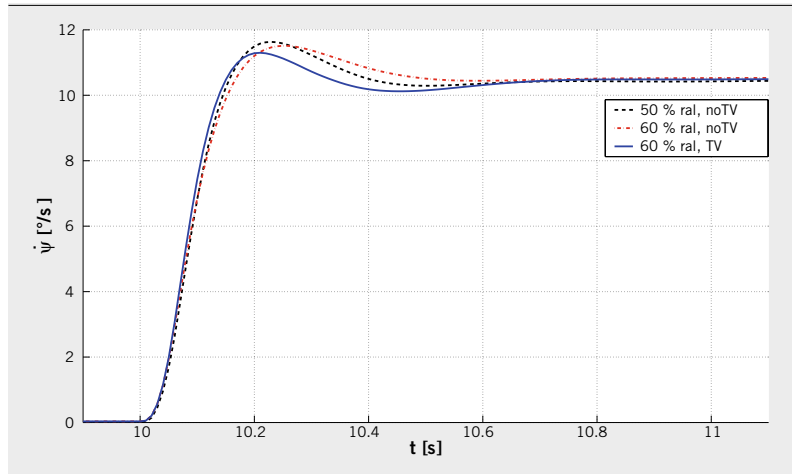
As reference value, a car with 50 % rear axle load is chosen (50 % ral) and its simulation results are compared with a car with tail-heavy axle load distribution (60 % ral), with and without torque vectoring (TV/ no TV). For this purpose, spring and damper characteristics are modified according to their respective load cases.

In 4, the course to steering wheel angle versus lateral acceleration is shown. As desired, a car with perfect (= even) axle load distribution provides a linear gradient at the beginning, progressively rising for higher lateral accelerations, even without torque vectoring (50 % ral, no TV). Increase of rear axle load (60 % ral, no TV) alters the driving behaviour towards less understeering. As the driving behaviour can be modified within a wide range, priority objective of this study was defined to emulate the static behaviour of the well-balanced car. Moreover, the reachable lateral acceleration was to be maximised. Simulation results show that up to medium lateral accelerations the driving behaviour of the reference car (50 % ral) is emulated via torque vectoring (60 % ral, TV) as the courses of the steering wheel angles are similar. For higher lateral accelerations, the torque vectoring influence is lowered to enable higher lateral accelerations.

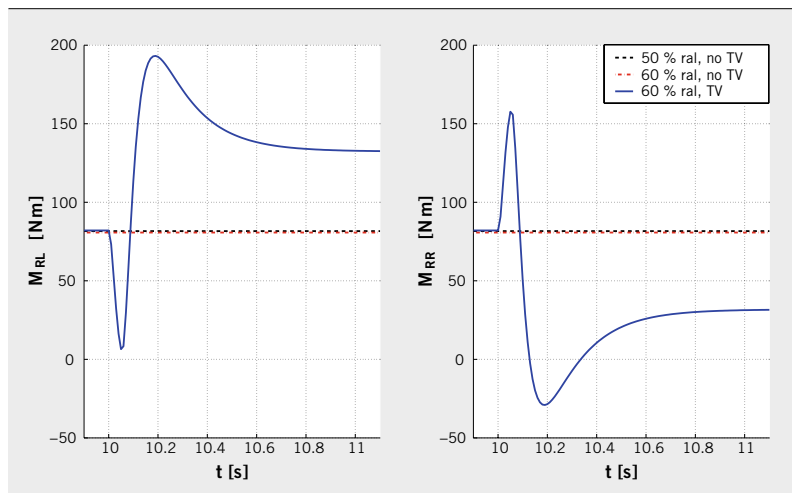
The corresponding wheel torques are shown in 5: Uncontrolled, the resulting lateral forces are almost independent on axle load distribution. With increasing lateral accelerations, higher vehicle speed is necessary, in addition, needed wheel slip angles are higher, which results in higher driving torques for overcoming driving resistances. Torque vectoring control shifts driving torques from the outer (right) to the inside wheel (left) and therefore counteracts unwanted yawing. For this reason, the driving tendency is modified towards understeering. For increasing lateral accelerations, this tendency is curve-based lowered dependent on lateral acceleration for not exceeding wheel-track adhesion limits and allowing higher lateral accelerations. Furthermore, excessive longitudinal wheel torques reduce the lateral force potential of the wheels, which exacerbates the oversteering tendency. Shifting wheel torque towards the outer wheel is not suitable in this case as the vehicle itself tends towards oversteering due to heavy rear axle load, hence an additional in-turning yaw moment destabilises the vehicle.

3.2 STEP-STEER

Dynamic response for transient steering wheel angles is investigated by the manoeuvre step-steer according to [12]. For this, the steering wheel angle is ramped up with a gradient of $500^\circ/\text{s}$ from zero to a value which correlates to a steady-state lateral acceleration of 4 m/s^2 . The initial longitudinal speed is set to 80 kph. The aim is to generate fast vehicle response characteristics with small values of overshoot and settle time. For better comparability of the different setups, two characteristic values are evaluated [13]: The peak-response-time T_{ψ} , which is defined as the time gap between the moment when 50% of the steering wheels' end value is reached ($T_{\delta_{\text{SWA}, 50\%}}$) and the moment when the yaw rate passes



7 Yaw rate versus time for step-steer



8 Wheel torques left and right for step-steer

90 % of its steady-state value ($T_{\psi 90\%}$). As second value, the overshoot value OS_{ψ} is evaluated through the yaw rates' steady-state value $\dot{\psi}_{stat}$ and its maximum $\dot{\psi}_{max}$. Both values are to be minimised [14], respective calculation formulas and simulation results for several vehicle configurations are given in 6.

The results for the yaw rate versus time for the step-steer manoeuvre are given in 7. The well-balanced car shows good driving behaviour with fast increase of the yaw rate and a small overshoot value. The tail-heavy car without torque vectoring shows inert behaviour: the overshoot value is smaller, the yawing response is less instantaneous. By the use of torque vectoring, the vehicles' response is considerably improved: Although the response time is improved even in comparison to the reference car, the overshoot value is the smallest of all configurations.

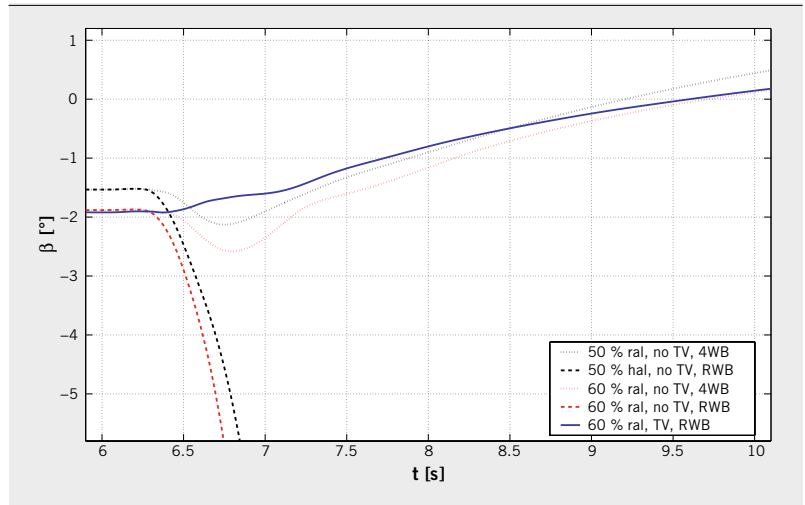
How this is achieved can be explained by the course of the wheel torques, 8: at the beginning of the manoeuvre the inner wheel (left) is decelerated, which results in an in-turning yaw moment. Wheel torque of the outer wheel (right) is increased by the same amount simultaneously to encourage yawing and to prevent changes of overall longitudinal forces. To compensate the subsequent overshoot of the vehicles' yaw rate, an out-turning, damping yaw moment is generated. Steady-state understeering is desired,

hence the steady-state end value of the inner wheel is chosen higher than for the outside wheel.

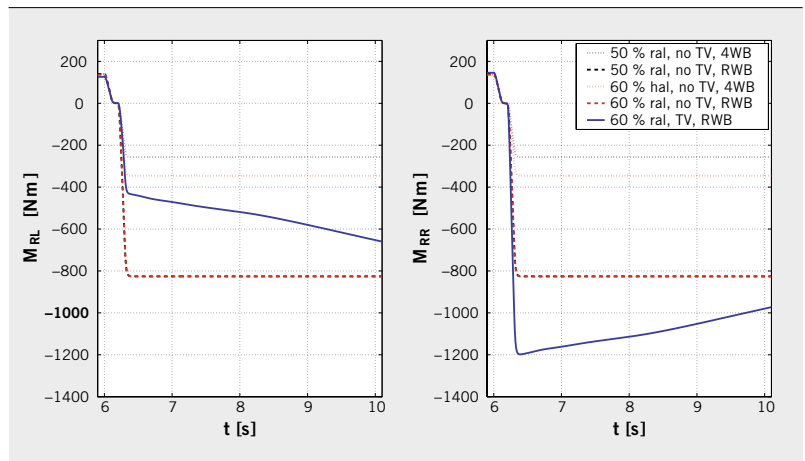
3.3 BRAKING WHILE CORNERING

A substantial challenge for establishing electro mobility is the increase of driving range. Therefore, recuperation should be used as much as possible when slowing down the vehicle for restoring kinetic energy. This means for a rear-driven electric vehicle, that as many driving situations as possible should be accomplished by only braking the rear wheels, which is a challenge especially when braking while cornering [15]. Therefore, investigations are focused on the driving stability for the manoeuvre braking while cornering as it is defined in [16]. At the beginning of the manoeuvre, the vehicle is steady-state cornering with an initial lateral acceleration of 7 m/s². At t = 6 s the driver changes from throttle to brake pedal and decelerates the car with 3.5 m/s². Full brake pressure is applied at t = 6.3 s. The radius is 100 m, the friction coefficient is chosen to be 1.0 (dry asphalt).

Within this manoeuvre, the advantages with respect to vehicle dynamics via torque vectoring become very clear: The lateral tyre force potential is reduced by dynamic axle load shift through braking as well as by applied longitudinal forces, which can lead to an



9 Side slip angle versus time for braking while cornering



10 Wheel torques of the inner wheel (left) and the outer wheel (right) during braking while cornering

in-turning tendency up to swerving of the vehicle. Shifting brake torque towards the outer wheel recuperative via torque vectoring causes two stabilising effects: First, the loss of lateral force due to longitudinal forces is reduced by the asymmetric distribution towards the wheel with higher overall tyre force potential. Second, an out-turning, stabilising yaw moment is generated, which prevents a spin-out. [17] pointed out the advantages achieved by torque vectoring for this manoeuvre for lower lateral accelerations on several friction coefficients for a controlled vehicle without mentioning the control structure and investigation of axle load distribution.

Most important stability criterion for this manoeuvre is the course of the side slip angle. Consequently, the behaviour of vehicles where brake torques are only applied to the rear wheel axes (RWB) are investigated as well as all-wheel braked cars with steady-state brake-force distribution (4WB). To objectively compare the results, the overshoot value OS_{β} is defined, which states the maximum deviation of the side slip angle from steady-state initial value.

The course of the side slip angle during the manoeuvre is shown in 9. Both all-wheel braked cars show stable driving behaviour. After a small overshoot ($OS_{\beta} = -0.595^{\circ}$, respectively -0.700°), the side slip angle is continuously reduced. By only braking the vehi-

cles rear wheels, the side slip angle rises excessively and the car spins out. By the use of torque vectoring, the car behaves very stable and easy controllable. The overshoot value OS_{β} is 0 as there is no overshoot of side slip angle, which states the almost perfect course of the side slip angle with maximisation of stability reserve.

Corresponding brake torques of the rear wheels are given in 10. All-wheel braked cars need less brake torques at the rear axle, whereby the loss of lateral wheel force potential is less and hence the driving situation remains save and stable. For zero-crossing of the wheel torque, the gradient is limited for protecting the gears from coming to harm. When braking only at the vehicles' rear wheels, the required brake torques are independent on the axle load distribution. In both cases without torque vectoring (50 % and 60 % rear axle load), the tyre force potential is exceeded and the car spins out. Above mentioned effects when shifting brake torque to the outer wheel provide stable deceleration of the vehicle, thus torque vectoring prevents the spin-out. Nevertheless, it has to be taken into account that higher lateral forces are needed at the vehicle's rear wheels compared to the all-wheel braked car, hence utilisation of the tyre force potential is higher which can lead to stability problems, e.g. for altering friction coefficient.

4 CONCLUSION AND OUTLOOK

Investigations for a vehicle concept with single rear wheel drive were made within this contribution. Installation-space optimised package of required drivetrain components can result in heavy rear axle loads which are challenging with respect to vehicle handling. Negative aspects of the unconventional axle loads can be compensated through torque vectoring: The steady-state driving behaviour is equalised with a reference behaviour with increase of achievable lateral acceleration. Improvement of agility and stability is shown with the manoeuvre step-steer. As especially critical but important manoeuvre, braking while cornering was investigated, where torque vectoring provides stability and driveability.

Previous results are achieved through simulation with high friction values. Therefore, capabilities of influencing driving dynamics via torque vectoring on lower friction coefficients are in focus of future investigations. For compensation of disturbances, the feedback controller will be activated. Furthermore, results will be confirmed in real vehicle tests.

REFERENCES

- [1] Mertens, A.: VDE-Studie Elektrofahrzeuge. Leibnitz, Universität Hannover, Forum "Life Needs Power", Hannover Messe Industrie, 22.04.2010
- [2] Biermann, J.-W.; Hartmann, B.: Maßgeschneiderte Fahrzeugkonzepte für Elektroantriebe. Drive-E-Akademie, Erlangen, 10.03.2010
- [3] Pruckner, A.: Vehicle Dynamics per Software – Potentials of an Electric Single Wheel Drive. Conference on Future Automotive Technology – Focus Electromobility. Wiesbaden: Springer-Verlag, 2013
- [4] Meissner, C.; Tenberge, P.: New concepts of Active Yaw Control for Electric and Hybrid Vehicles. Proceedings of the third international Conference on Mechanical Engineering and Mechanics (ICMEM), Beijing, 21.-23.10.2009
- [5] Billing, C.; Boedrich, H.; Brack, J.; Höll, B.; Holle, M.; Kimmich, F.: Die Dynamic Performance Control von BMW. In: ATZ 110 (2008), No. 11, pp. 984-994
- [6] Klomp, M.: Longitudinal Force Distribution and Road Vehicle Handling. Gothenburg, Chalmers University of Technology, Dissertation, 2010
- [7] Folke, R.; Böker, R.; Thomys, A.; König, L.: Torque Vectoring – Ein neuer Freiheitsgrad bei E-Fahrzeugen. In: ATZ 112 (2010), No. 6, pp. 404-408
- [8] Kaiser, G.; Holzmann, B.; Korte, M.; Werner, H.: Torque Vectoring with a Feedback and Feed Forward Controller – Applied to a through the Road Hybrid Electric Vehicle. IEEE Intelligent Vehicle Conference, Karlsruhe, 2011
- [9] Kaspar, S.; Pruckner, A.; Stroph, R.; Hohmann, S.: Potential of vehicle dynamics via single wheel drive for installation space optimized electric vehicles, Aachener Kolloquium Fahrzeug- und Motorentechnik, Aachen 2012
- [10] Pacejka, H.: Tire and Vehicle Dynamics. Oxford: Butterworth-Heinemann, 2006
- [11] DIN ISO 4138: Straßenfahrzeuge – Stationäre Kreisfahrt, Deutsches Institut für Normung e.V., Berlin, 1984
- [12] DIN ISO 7401: Straßenfahrzeuge – Testverfahren für querdynamisches Übertragungsverhalten, Deutsches Institut für Normung e.V., Berlin, 1989
- [13] Mitschke, M.; Wallentowitz, H.: Dynamik der Kraftfahrzeuge. Berlin: Springer-Verlag, 2004
- [14] Greger, M.: Auswirkungen einer variablen Momentenverteilung auf die Fahrdynamik, Dissertation, TU München, 2006
- [15] Schönemann, B.; Henze, R.; Küçükay, F.; Kudritzki, D.: Auswirkung der Rekuperation auf die Fahrdynamik. In: ATZ 115 (2013), No. 6, pp. 520-527
- [16] DIN ISO 7975: Bremsen in der Kurve: Testverfahren im offenen Regelkreis, Deutsches Institut für Normung e.V., Berlin, 1987
- [17] Graf, M.; Wiesbeck, F.; Lienkamp, M.: Fahrdynamikauslegung des Elektrofahrzeugs MUTE. In: ATZ 113 (2011), Nr. 6, pp. 452-457